

A SYSTEM FOR TESTING AIRDATA PROBES AT HIGH ANGLES OF ATTACK USING A GROUND VEHICLE

Robert J. Geenen*
 NASA Ames Research Center
 Dryden Flight Research Facility
 P.O. Box 273
 Edwards, CA 93523-0273

Bryan J. Moulton**
 NASA Ames Research Center
 Dryden Flight Research Facility
 P.O. Box 273
 Edwards, CA 93523-0273

Advisor: Edward A. Haering Jr.**
 NASA Ames Research Center
 Dryden Flight Research Facility
 P.O. Box 273
 Edwards, CA 93523-0273

Abstract

A system to calibrate airdata probes at angles of attack between 0° and 90° was developed and tested at the NASA Ames Research Center, Dryden Flight Research Facility. This system used a test fixture mounted to the roof of a ground vehicle and included an onboard instrumentation and data acquisition system for measuring pressures and flow angles. The data could be easily transferred to the facility mainframe computer for further analysis. The system was designed to provide convenient and inexpensive airdata probe calibrations for projects which require airdata at high angles of attack, such as the F-18 High Alpha Research Program. Previous subsonic data for the NACA standard pitot-static tube with vane-type flow direction indicators was limited to 20° angle of attack. This type of probe was tested to 90° angle of attack in a wind tunnel and using the ground vehicle system. The results of both tests are in close agreement. An airdata probe with a swiveling pitot-static tube was also calibrated with the ground vehicle system. This paper presents the results of these tests and gives a detailed description of the test system.

Nomenclature

D	diameter of pitot-static tube, ft
E_s	static pressure error, $\frac{P_{s_i} - P_{s_{\infty}}}{q_c} \times 100$, percent
E_t	total pressure error, $\frac{P_{t_i} - P_{t_{\infty}}}{q_c} \times 100$, percent
HARV	high alpha research vehicle
NACA	National Advisory Committee on Aeronautics

*Aeronautical Engineer. Member AIAA.

**Aerospace Engineer.

Copyright ©1990 by the American Institute of Aeronautics and Astronautics, Inc. No copyright is asserted in the United States under Title 17, U.S. Code. The U.S. Government has a royalty-free license to exercise all rights under the copyright claimed herein for Governmental purposes. All other rights are reserved by the copyright owner.

P_{s_i}	indicated static pressure (measured on test probe), lbf/ft ²
$P_{s_{\infty}}$	true static pressure (measured on reference probe), lbf/ft ²
P_{t_i}	indicated total pressure (measured on test probe), lbf/ft ²
$P_{t_{\infty}}$	true total pressure (measured on reference probe), lbf/ft ²
q_c	impact pressure, $P_{t_{\infty}} - P_{s_{\infty}}$, lbf/ft ²
RN_{α}	Reynolds number normal to probe, $\frac{\rho V_i D}{\mu} \sin(\alpha_i)$
u, v, w	three components of airspeed in noseboom axes system, ft/sec
V_i	true airspeed, mi/hr
α	angle of attack, deg
α_i	indicated angle of attack, $\tan^{-1}[\frac{w}{u}]$, deg
β_i	indicated angle of sideslip, $\tan^{-1}[\frac{v}{u}]$, deg
Δ	differential
ν	kinematic viscosity of air, sec/ft ²

Introduction

In recent years a great deal of interest has been expressed in high-angle-of-attack flight. This interest led to high-angle-of-attack research projects on the F-18 and X-29 aircraft at the NASA Ames Research Center, Dryden Flight Research Facility. The results obtained from these projects pointed out the deficiencies of current airdata probes in providing accurate information at high angles of attack (greater than 30°). The standard NACA combined pitot-static tube with vane-type flow direction indicators¹ has proven quite effective for normal flight conditions. However its characteristics in subsonic flow were unknown beyond +20° angle of attack for static pressure¹ and ±45° angle of attack for to-

tal pressure.² A complete calibration (0° to 90° angle of attack) of this probe was necessary to determine its usefulness at high angles of attack. To provide data on this and other airdata probes an effort was undertaken in support of the high-angle-of-attack research projects conducted at NASA Ames-Dryden.

Wind tunnels have been the most common means for calibrating airdata probes. But wind tunnels are expensive to operate and require a great deal of advanced notice and planning to schedule tests. A simple, low-cost, accurate system for calibrating airdata probes at high angle of attack was desired. A system was proposed which used a fixture mounted to the roof of a ground vehicle to position a test probe and a reference probe in the flow field above and in front of the vehicle. The test probe orientation could be varied from 0° to 90° angle of attack. The speed of the ground vehicle was adequate to simulate Reynolds numbers seen in low-speed, high-angle-of-attack flight.

The accuracy of the ground vehicle system was verified by comparing results obtained using the ground vehicle system and various wind tunnels. Wind-tunnel tests were completed in 1959¹ for an entire NACA probe at low angles of attack (up to 20°), in 1951² for the total pressure port alone to moderate angles of attack ($\pm 45^\circ$), and in 1989 in the NASA Langley 14- by 22-ft Subsonic Wind Tunnel (Haering, E. A. Jr., and Banks, D.W., NASA Technical Memorandum, to be published) for the entire NACA probe at high angles of attack (up to 90°). The conditions for the probe calibration using the Langley wind tunnel were: maximum dynamic pressure of 130 lb/ft^2 , unit Reynolds numbers between 700,000 and 2,000,000 /ft, and Mach numbers between 0.100 and 0.300.

The system also was used to determine the characteristics of the static and total pressure error as a function of indicated angle of attack for two different airdata probes. A standard NACA airdata probe and a swiveling-head airdata probe were tested.

This report contains: (1) a detailed description of the ground vehicle system and its use, (2) a comparison of ground vehicle to wind-tunnel data, and (3) calibration results of a standard NACA airdata probe and a swiveling-head airdata probe. The NACA airdata probe was calibrated between 0° and 90° angle of attack while the swiveling head-airdata probe was calibrated between -14° and 150° angle of attack. The ground vehicle probe calibrations were done at a ground speed of 60 mi/hr and an altitude of 2,300 ft above sea level. This resulted in a dynamic pressure of 8 lb/ft^2 , a unit Reynolds number of 550,000 /ft, and a Mach number of 0.075.

Description of Apparatus

Ground Vehicle and Support Structure

The main component of the ground vehicle system was the probe support structure, shown in Fig. 1. This structure allowed for placement of a reference probe and a test probe in a variety of positions and attitudes. The reference probe was a standard NACA airdata probe. It could be positioned over a large rectangular area on the starboard side of the vehicle (a standard van) but remained constantly aligned with the free stream. The test probe was located on the port side of the vehicle and pivoted horizontally on a large protractor toward the centerline of the vehicle, as shown in Fig. 2. Note that the test probe must be rotated 90° (about its longitudinal axis) from its normal aircraft attitude for the horizontal rotation to provide angle of attack. The test probe may also be rotated about its longitudinal axis to provide angle of sideslip. All of these adjustments are manual, therefore only steady-state tests may be done using this system.

The distance between the probes and the vehicle was maximized while attempting to keep the structure a reasonable size and weight. The exact dimensions of the structure and its proximity to the vehicle are shown in Fig. 3. During calibration, the probes were 115.5 in. above the ground and 36.5 in. above the roof line. The tip of the NACA test probe was 45.6 in. in front of the vehicle at angle of attack (α) = 0° and 6.6 in. at $\alpha = 90^\circ$. The reference probe tip was 45.6 in. in front of the vehicle and 34 in. off of the centerline of the vehicle.

Airdata Probes

The reference probe, and one of the probes calibrated using the ground vehicle system were both standard NACA airdata probes. A standard NACA probe, shown in Fig. 4, consists of a combined pitot-static tube with vane-type flow-angle indicators. The flow-angle measuring components consist of mass-balanced vanes which are free to pivot about mounting posts perpendicular to the probe centerline. Potentiometers mounted inside the probe provide analog output of the vane position. Details of the total and static pressure port geometry are shown in Fig. 5.

The other probe calibrated was a swiveling-head airdata probe, shown in Fig. 6. This probe consisted of a combined pitot-static tube with four alignment fins attached to the aft-end of the tube. This entire assembly was attached to the remainder of the probe by a gimbal mechanism. This arrangement allowed the pitot-static tube to swivel freely within a certain range, as illustrated in Fig. 7. The tube was mass balanced about the gimbal allowing the vanes to maintain alignment with the flow. The remainder of the probe consisted of the gooseneck attached to the gimbal, and flow direction indicators identical to those used on the NACA airdata probe. The swivel probe, however, used synchros instead of potentiometers to determine the orientation of the flow direction indicators.

Instrumentation

The instrumentation for this system was designed to be flexible enough to accommodate many different types of probes. A typical probe has four parameters to measure: indicated total pressure (P_{t_i}), indicated static pressure (P_{s_i}), indicated angle of attack (α_i), and indicated angle of sideslip (β_i). These parameters are also measured on the reference probe to give true total pressure (P_{t_∞}), true static pressure (P_{s_∞}), α_i , and β_i . The instrumentation system consisted of the transducers listed in Table 1, along with the appropriate signal conditioning and an onboard computer for data storage.

The six differential pressure transducers were arranged as shown in Fig. 8. Four of the transducers had one side exposed to ambient pressure, which was measured by the absolute pressure transducer. Combining ambient pressure data with differential pressure data allowed the absolute total and absolute static pressure for each probe to be determined. Two additional differential pressure transducers, one between the total ports of each probe and one between the static ports of each probe, added both sensitivity and redundancy to the system.

The onboard computer was used to control the sample rate and data storage. This computer had approximately 153 k of memory. This provided approximately 2 min of data storage at 50 samples/sec on 11 channels for a typical probe calibration.

Support Equipment

To calibrate an airdata probe several peripheral pieces of equipment were necessary, including a fifth-wheel ground-speed and distance indicator, an anemometer, and a thermometer. The fifth wheel was mounted on the rear of the vehicle and the anemometer and thermometer were attached to the support structure as shown in Fig. 9. The fifth-wheel equipment included two digital displays (distance and speed) located directly in front of the driver. The fifth-wheel distance display was calibrated by rolling it over known distance marks on the ground and then adjusting the wheel diameter (by inflation or deflation) appropriately. The speed display received input from the distance display and was assumed to be correct if the distance was correct. The speed display was used by the driver to assist in maintaining the desired ground speed. The anemometer was used for measuring the wind speed between calibration runs. The wind speed was monitored to make certain that it stayed within acceptable limits. The thermometer was used to monitor the ambient air temperature so that airspeed and Reynolds number could be calculated.

Flow Quality and Sensor Accuracy

Flow-Field Survey

To determine the steady-state environment in which the test probe would be calibrated, a survey of the flow field in

front and above the ground vehicle was taken. The survey was accomplished by using the reference probe to sample a matrix of points in the flow field. The reference probe measured the variations in both upwash and sidewash caused by the ground vehicle and the support structure.

The same hardware arrangement used for probe calibrations was used for the survey, with the exception of a test probe. The test probe was absent during the survey so that the flow field and its causes were determined accurately.

The results of the survey identified the area of least upwash. This area had an upwash angle that varied between 6.5° and 8° and was chosen as the optimal placement for the reference probe. The area of the flow field in which the test probe was placed during calibrations had an upwash angle that ranged from 9° to 14° . There was no compensation for the errors induced by the upwash of the ground vehicle. No corrections were made for position error from compressibility because of the low Mach number of the ground vehicle.

Transducer Calibrations

A combination of the sensors' operating ranges and the capabilities of the onboard digital computer determined the resolution to which the data could be measured. The transducers were of a linear design and a least squares linear curve fit was used for the resulting calibration. Table 1 shows the resolution and accuracy of each of the transducers as connected to the onboard digital computer through the signal conditioning hardware.

Airdata Probe Calibration Techniques

Details of System Operation

A standard probe calibration consisted of a range of test points between 0° and 90° angle of attack, in 5° increments. The probe calibration could be conducted on any straight, level surface approximately one mile in length. At each angle of attack, 30 sec of stabilized data were collected traveling in one direction. Another 30 sec of data were then collected traveling in the opposite direction. The heading is not important as long as it is held constant. The reciprocal headings confirm the repeatability of the test data and identify any wind effects. To minimize the error introduced by the wind, a wind limitation of 5 kn was set. A crosswind of 5 kn induces a 5.5° angle of attack on the reference and test probes when the vehicle is traveling at 60 mi/hr. This was the speed where all calibrations were conducted.

A standard probe calibration took several hours to complete. Unfortunately, the differential pressure transducers showed a significant temperature sensitivity, so approximately every 30 min pressure tares were taken. Postcalibration analysis used this tare information to correlate the instrumentation's drift with time. This, in turn allowed for the correction of the calibration data during the data reduction process.

Data Reduction

Total pressure error (E_t), is defined as the percentage of impact pressure that the test probe's total pressure is greater than the reference probe's total pressure,¹ and static pressure error (E_s), is defined as the percentage of impact pressure that the test probe's static pressure is greater than the reference probe's static pressure.¹ In equation form this is

$$E_t = \frac{Pt_i - Pt_{\infty}}{q_c} \times 100 \quad (1)$$

$$E_s = \frac{Ps_i - Pt_{\infty}}{q_c} \times 100 \quad (2)$$

These two errors should be a function only of α_i and β_i on the test probe for the incompressible Mach numbers and subcritical Reynolds numbers used for conducting the test.

Each 30-sec calibration run is analyzed using the following procedure. Time histories of seven parameters, α_i and β_i on the reference probe, α_t and β_t on the test probe, airspeed (V_t), as calculated from the reference probe and temperature, E_t , and E_s were inspected. A time interval of several seconds was identified where all seven of the parameters were at a stabilized condition. This time interval was used as the data point for that particular run. The errors in total and static pressure were associated with the angle of attack measured by the test probe at that point. The overview of the group of parameters was to insure that the data point was at a stabilized condition and the measurements were not being affected by a wind gust or heading adjustment. Figure 10 shows a sample of the seven parameters during a time interval chosen for that particular data point.

Results and Discussions

Applicability of Results

One project objective was to develop a system for calibrating airdata probes at high angle of attack. To apply these calibrations to flight vehicles, it was necessary to conduct the test within the same Reynolds number range as that seen in low speed, high-angle-of-attack flight. The Reynolds number used is based on probe diameter and the component of velocity normal to the longitudinal axis of the cylinder:³

$$RN_{\alpha} = \frac{V_t D}{\nu} \sin(\alpha_i) \quad (3)$$

A typical high-angle-of-attack maneuver for the F-18 high alpha research vehicle (HARV) (Fig. 11) would generate an RN_{α} for its NACA airdata probe of 0 and 50,000 at 0° and 90° angle of attack, respectively. The ground vehicle system is capable of producing an RN_{α} for the NACA probe between 0 and 40,000 for angles of attack between 0° and 90°, respectively, at a ground speed of 60 mi/hr. In flight and on the ground vehicle, RN_{α} is well below the critical Reynolds number for that probe, as shown in Fig. 12.³

Verification of System Accuracy

To verify the accuracy of the system, results of several wind-tunnel tests, cited previously in the Introduction section, were compared with the ground vehicle system results for the calibration of a standard NACA airdata probe. Figures 13 and 14 show the wind-tunnel and ground vehicle system data overplotted for comparison.

The variation in total pressure error with angle of attack is shown in Fig. 13. The 1951 and 1959 data agree with the ground vehicle system data within approximately 1 percent over the entire range of angle of attack tested. The 1989 wind-tunnel data show a 2 percent bias at the low angles of attack which possibly resulted from the use of a small pitot tube located near the floor of the tunnel as a reference. The ground vehicle system calibration, as well as the two earlier wind-tunnel calibrations, used indicated total pressure at $\alpha = 0^\circ$ as a reference.

The variation in static pressure error with angle of attack is shown in Fig. 14. Unexplained scatter in the ground vehicle system data at low angles of attack makes the comparison difficult. However, the ground vehicle data lie between the 1959 wind-tunnel data and the 1989 wind-tunnel data over the entire angle-of-attack range tested.

Probe Calibration Results

Two airdata probes were calibrated using the ground vehicle system. The first probe calibrated was a standard NACA airdata probe. The variation in total pressure error with angle of attack is shown in Fig. 15. The total pressure error remains within 1 percent of impact pressure (q_c) for angles of attack between 0° and 30°. This agrees with references 1 and 2. After reaching $\alpha = 30^\circ$, the error in total pressure increases greatly (in the negative direction) reaching a value of -200 percent of q_c at $\alpha = 90^\circ$.

The variation in static pressure error with angle of attack is shown in Fig. 16. For unknown reasons the scatter in the data was much larger at the low angles of attack than at the high angles of attack. Over the entire angle-of-attack range tested, the error in static pressure stayed within 20 percent of q_c . The error in static pressure remained within approximately ± 5 percent of q_c for angles of attack between 0° and 50°. As angle of attack increased above 50°, the error in static pressure increased and reached 20 percent of q_c at 90°.

The ground vehicle system was also used to calibrate a swiveling-head airdata probe. Data were taken with the pitot-static tube free-floating and with the probe body at $\alpha = 0^\circ$. These data showed that the error in total pressure was zero and the error in static pressure was 4 percent as compared to the reference NACA airdata probe. In the region of angle of attack and angle of sideslip where the pitot-static tube could swivel freely, the error was thus assumed to be constant. Outside of this region the probe could not swivel freely and thus became inclined to the flow. The error

in this region was determined by locking the pitot-static tube so that it could not swivel with respect to the probe body and then giving the entire probe an angle-of-attack range. With the probe body at $\alpha = 0^\circ$, the errors were the same (within the accuracy of the system) with the pitot-static tube either free or locked.

The variation in total pressure error with angle of attack for the unlocked swivel probe is shown in Fig. 17. Note that the flat part of the curve between -14° and 73° angle of attack is because of the assumption that the error is the same wherever the probe is free to swivel. The error in total pressure remains at approximately 4 percent of q_c up to 100° . Beyond $\alpha = 100^\circ$ the error in total pressure increases greatly (in the negative direction) with increasing angle of attack.

The variation in static pressure error with angle of attack for the unlocked swivel probe is shown in Fig. 18. This shows a trend similar to that seen for total pressure. The static pressure error remains at approximately 4 percent of q_c until reaching $\alpha = 75^\circ$. At this point the static pressure error increases greatly (in the negative direction) reaching -57 percent of q_c at $\alpha = 140^\circ$. The static pressure error begins to decrease slightly after $\alpha = 140^\circ$ to -49 percent of q_c at $\alpha = 150^\circ$.

Figures 19 and 20 show a comparison between the NACA probe calibration and the swivel probe calibration. The swivel probe has a greater range of insensitivity to angle of attack than does the NACA probe. This makes the swivel probe better suited to high-angle-of-attack flight than the NACA probe.

Concluding Remarks

At the NASA Ames Research Center, Dryden Flight Research Facility, a system was developed to measure the total and static pressure errors of airdata probes up to angle of attack (α) = 90° . A ground vehicle was used as an alternative to wind-tunnel testing. The results obtained from this system are applicable to low-speed, high-angle-of-attack flight because the test was conducted at an incompressible Mach number and at Reynolds numbers comparable to flight.

The quality of data gathered by the system was verified by comparing the calibration of a standard NACA airdata probe from the ground vehicle system to wind-tunnel tests of the same airdata probe. Total pressure error measured by the ground vehicle system agreed to within 1 percent of the error measured during two wind-tunnel tests where the same error calculation method was used. Static pressure error data measured by the ground vehicle system lie between the data from two wind-tunnel tests.

Total and static pressure errors as a function of indicated angle of attack were measured for a standard NACA airdata probe and a swiveling-head airdata probe. Both of the probes were used on the F-18 high alpha research ve-

hicle (HARV). The swiveling pitot-static tube was locked in-position to determine its errors after the tube reached its mechanical stops. The total pressure error for the NACA airdata probe was less than 1 percent of impact pressure (q_c) up to $\alpha = 30^\circ$, and rapidly increased to -200 percent of q_c at $\alpha = 90^\circ$. The total pressure error of the swiveling-head probe was -4 percent of q_c up to $\alpha = 100^\circ$ and increased to -180 percent of q_c at $\alpha = 150^\circ$. The static pressure error of the NACA probe was less than 5 percent of q_c up to $\alpha = 50^\circ$, and increased rapidly to 20 percent of q_c at $\alpha = 90^\circ$. For the swiveling-head probe, static pressure error remained at approximately -4 percent of q_c until reaching $\alpha = 75^\circ$, then it increased greatly, reaching -57 percent of q_c at $\alpha = 14^\circ$. It then decreased to -49 percent of q_c at $\alpha = 150^\circ$.

The swiveling-head airdata probe's large region of total and static pressure insensitivity to angle of attack and angle of sideslip make it more suitable for high-angle-of-attack flight than the standard NACA airdata probe.

References

- ¹Richardson, Norman R., and Pearson, Albin O., *Wind-Tunnel Calibrations of a Combined Pitot-Static Tube, Vane-Type Flow-Direction Transmitter, and Stagnation-Temperature Element at Mach Numbers From 0.60 to 2.87*, NASA TN D-122, Oct. 1959.
- ²Gracey, William, Letko, William, and Russell, Walter R., *Wind-Tunnel Investigation of a Number of Total-Pressure Tubes at High Angles of Attack*, NACA TN-2331, Apr. 1951.
- ³Burnsall, William J., and Loftin, Laurence K., Jr., *Experimental Investigation of the Pressure Distribution About A Yawed Circular Cylinder in the Critical Reynolds Number Range*, NACA TN-2463, Sept. 1951.

Table 1. Transducer resolutions and accuracies.

Sensors	Resolution	Accuracy
Pressure-Differential		
Total (reference), lbf/ft ²	0.080	± 0.14
Static (reference), lbf/ft ²	0.019	± 0.12
Total (test), lbf/ft ²	0.073	± 0.23
Static (test), lbf/ft ²	0.085	± 0.14
Δ Total	0.158	± 0.22
Δ Static	0.076	± 0.04
Pressure-Absolute		
Ambient, lbf/ft ²	0.014	± 0.50
Flow Direction		
α_i (reference), deg	0.30	± 0.25
β_i (reference), deg	0.31	± 0.40
α_i (test), deg	0.21	± 0.45
β_i (test), deg	0.03	± 0.35

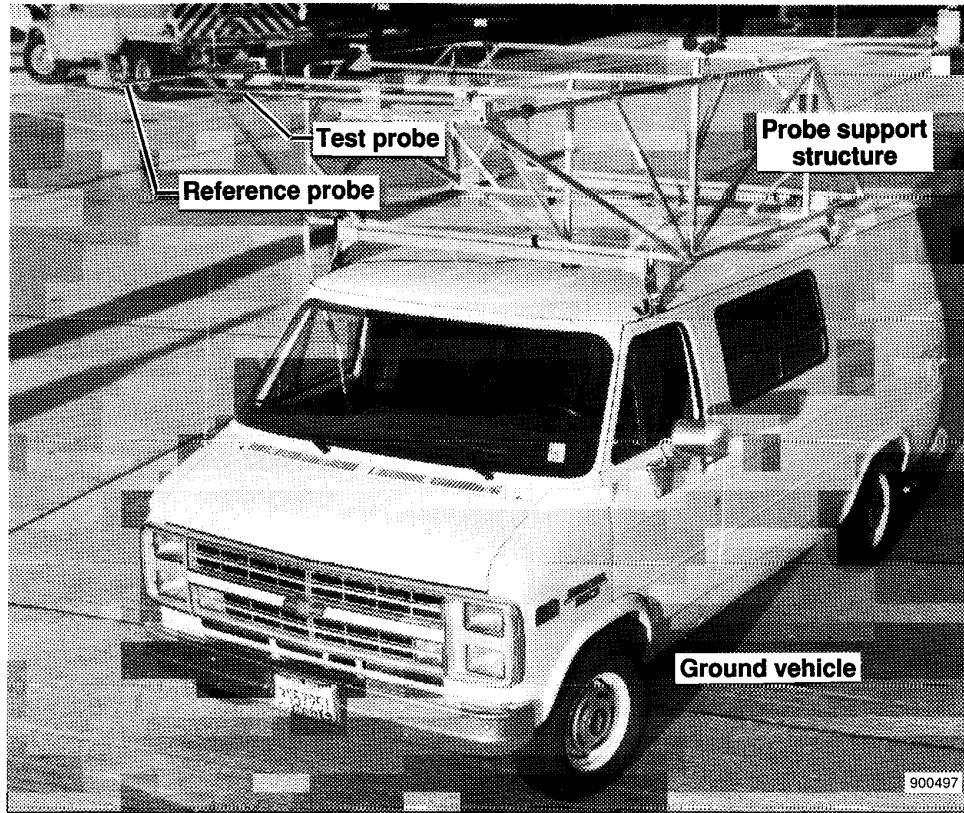


Fig. 1 Ground vehicle with probe support structure and airdata probes.

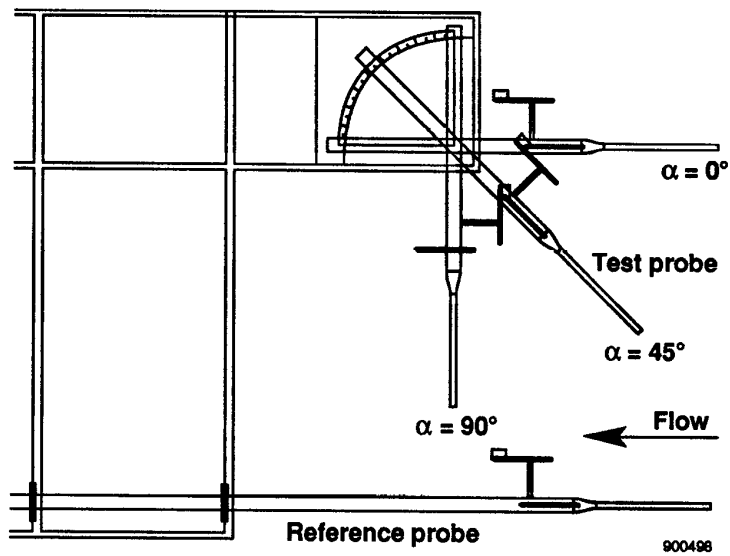


Fig. 2 Top view of probe support structure.

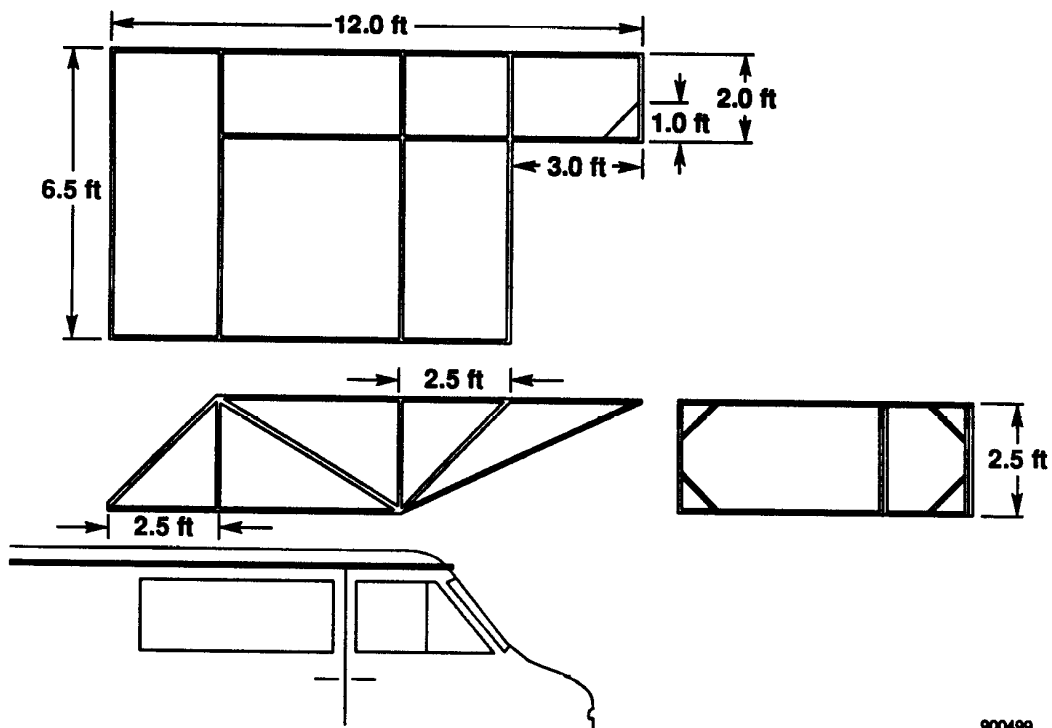


Fig. 3 Probe support structure with ground vehicle.

900499

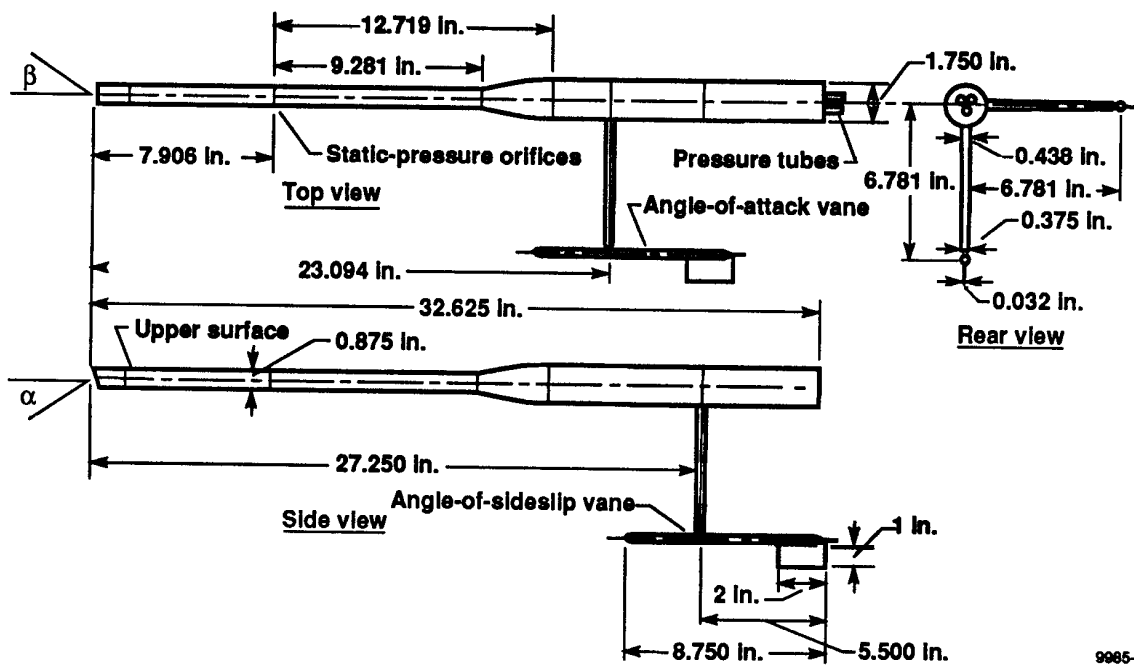
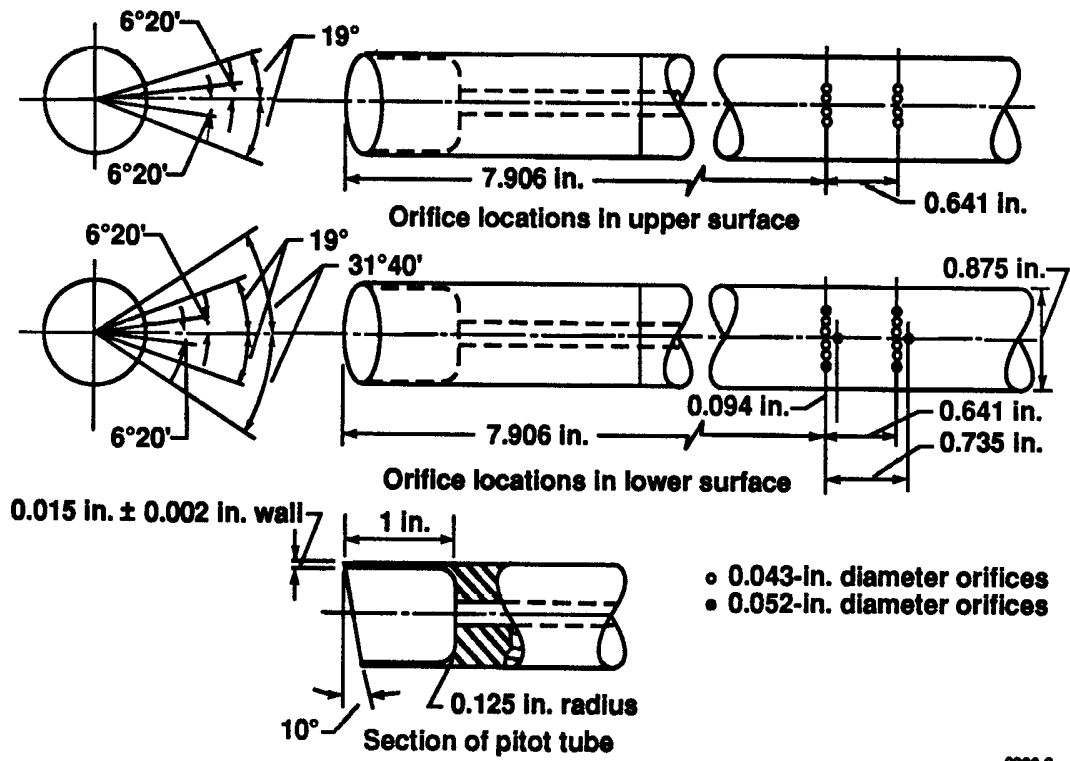


Fig. 4 Three views of the standard NACA airdata probe.

9985-2



9000-2

Fig. 5 Standard NACA airdata probe port configuration.

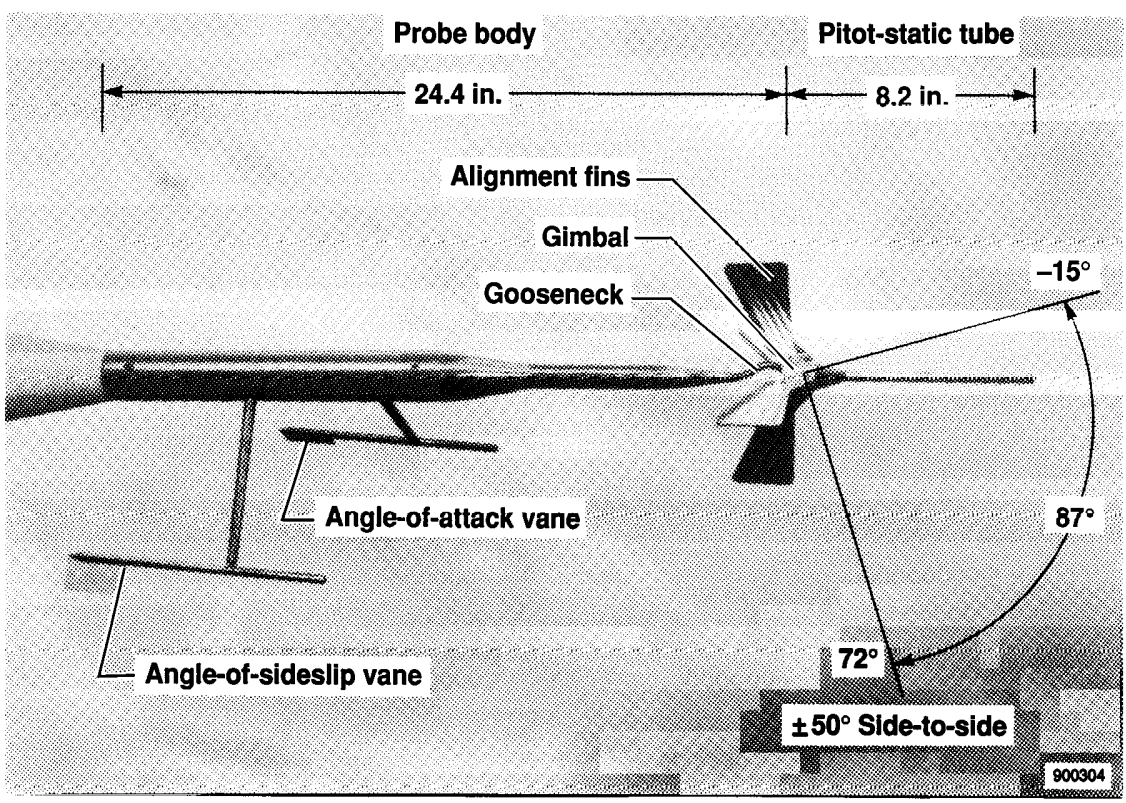


Fig. 6 Swiveling-head airdata probe.

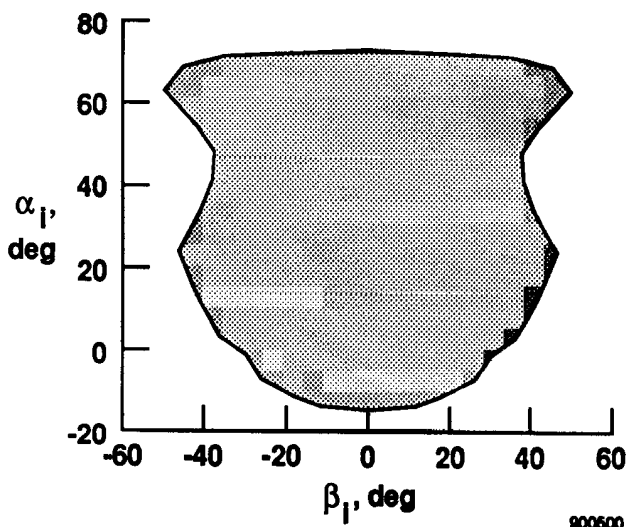


Fig. 7 Swivel probe range of motion.

900600

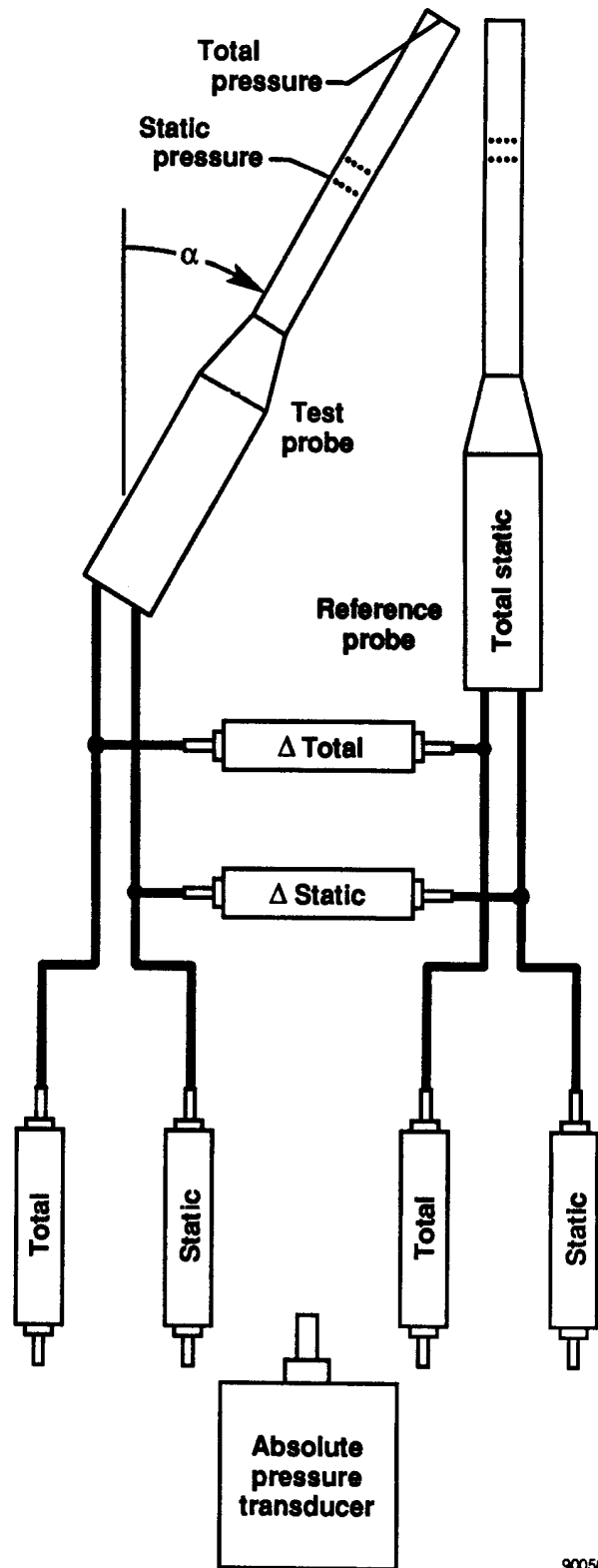


Fig. 8 Pressure transducer arrangement.

900501

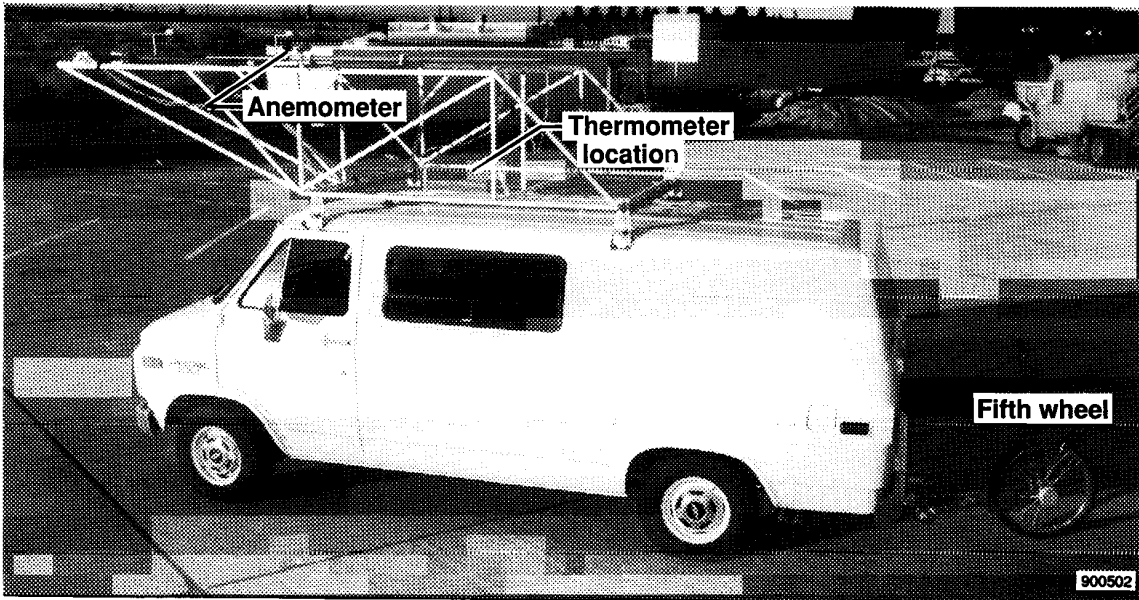


Fig. 9 Ground vehicle with support equipment.

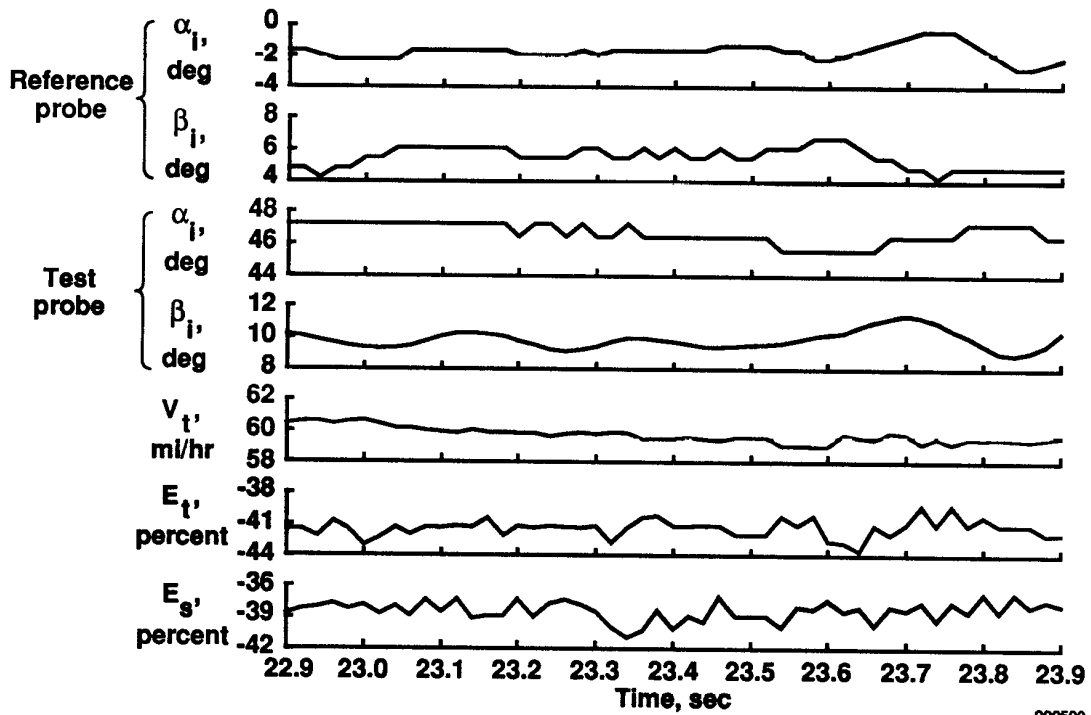


Fig. 10 Time history of calibration run.

900503

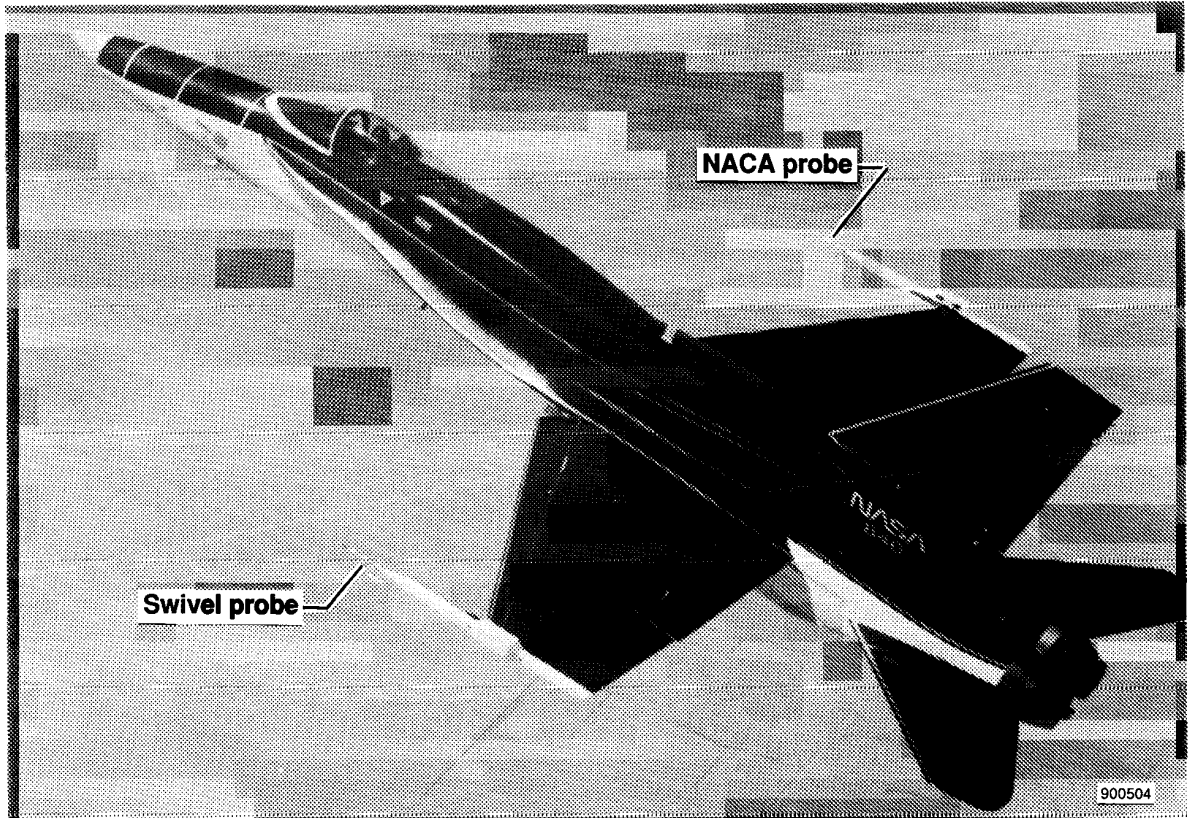


Fig. 11 F-18 HARV with NACA probe and swivel probe.

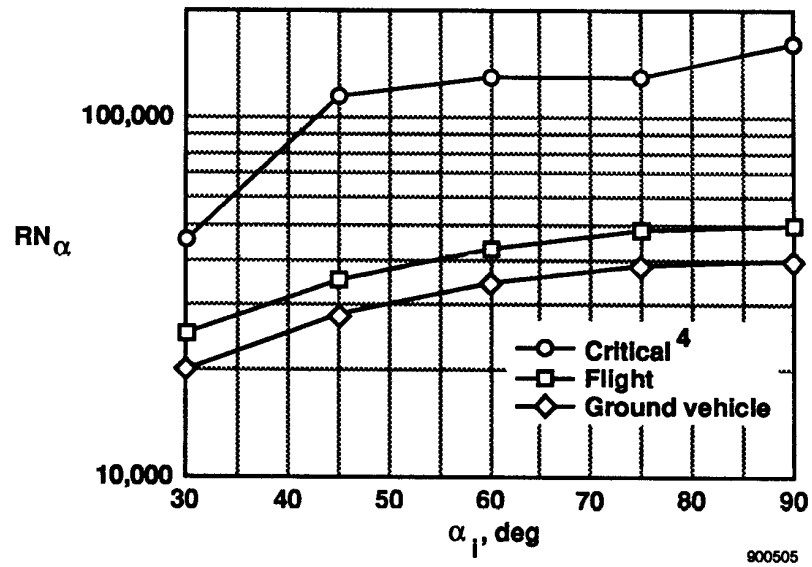


Fig. 12 Reynolds number as a function of angle of attack.

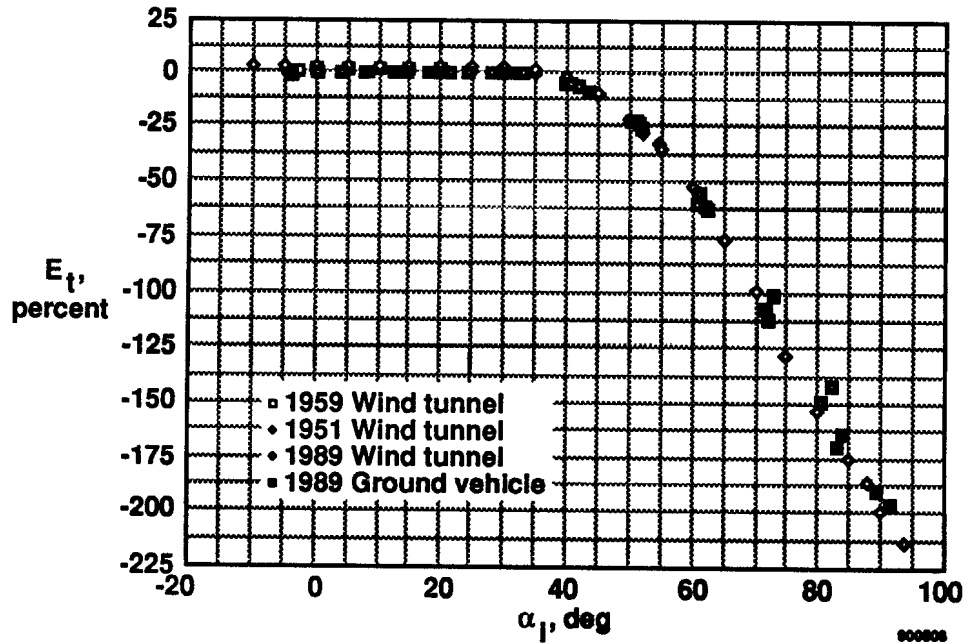


Fig. 13 NACA probe total pressure error.

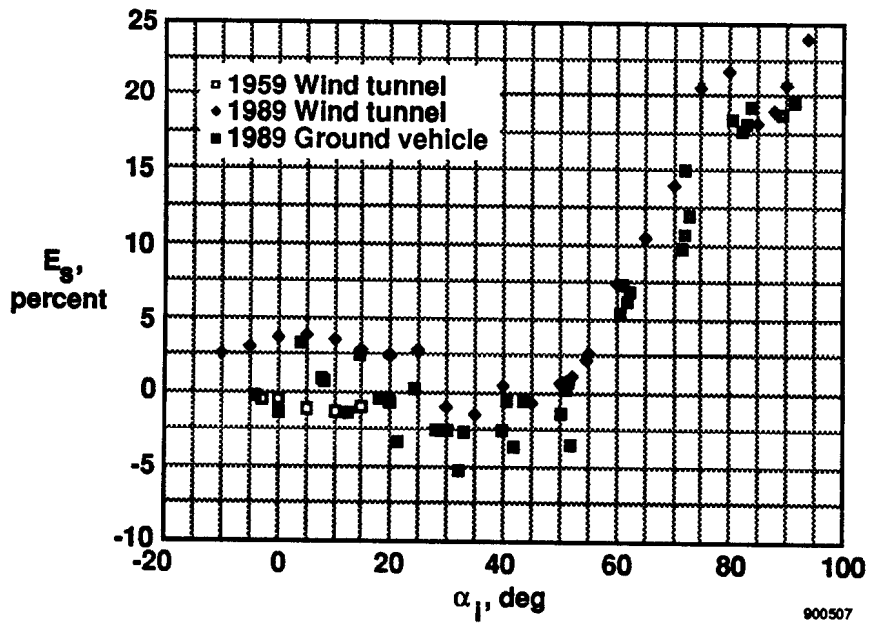


Fig. 14 NACA probe static pressure error.

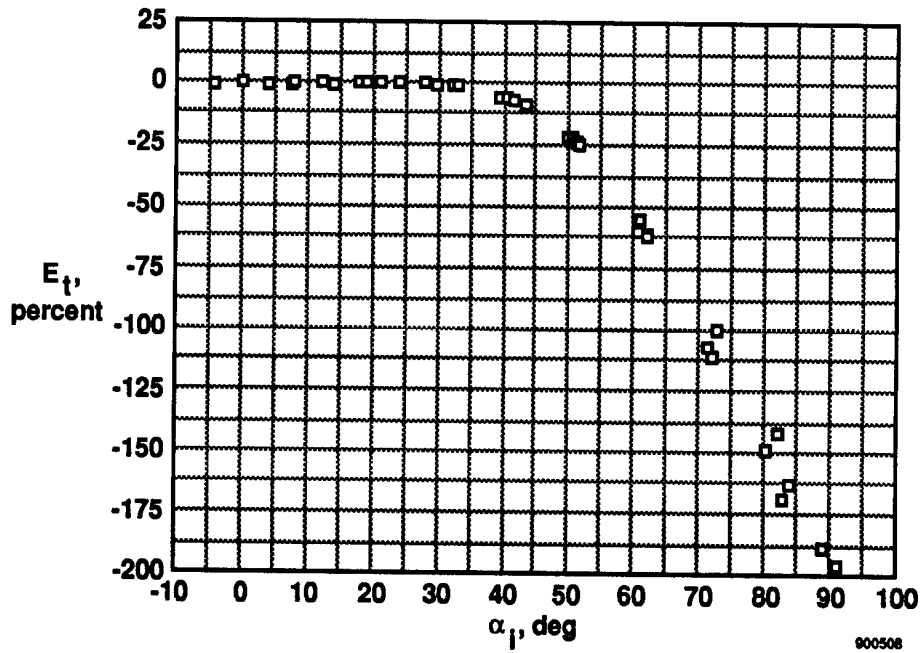


Fig. 15 NACA probe total pressure error (ground vehicle system).

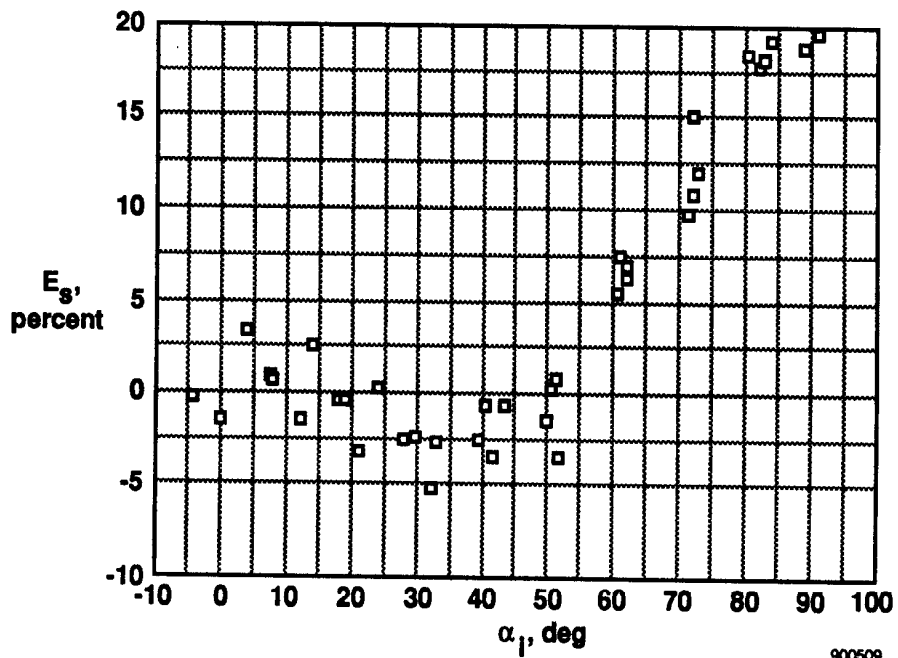


Fig. 16 NACA probe static pressure error (ground vehicle system).

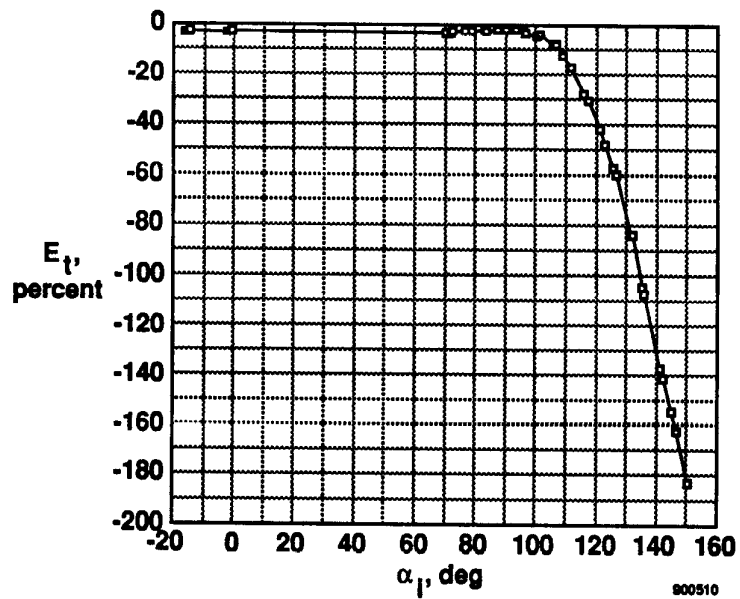


Fig. 17 Swivel probe total pressure error.

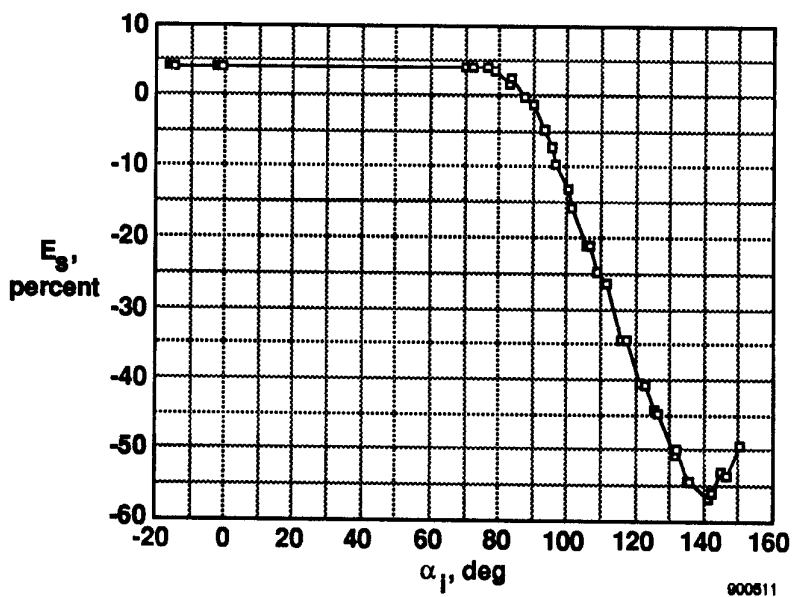


Fig. 18 Swivel probe static pressure error.

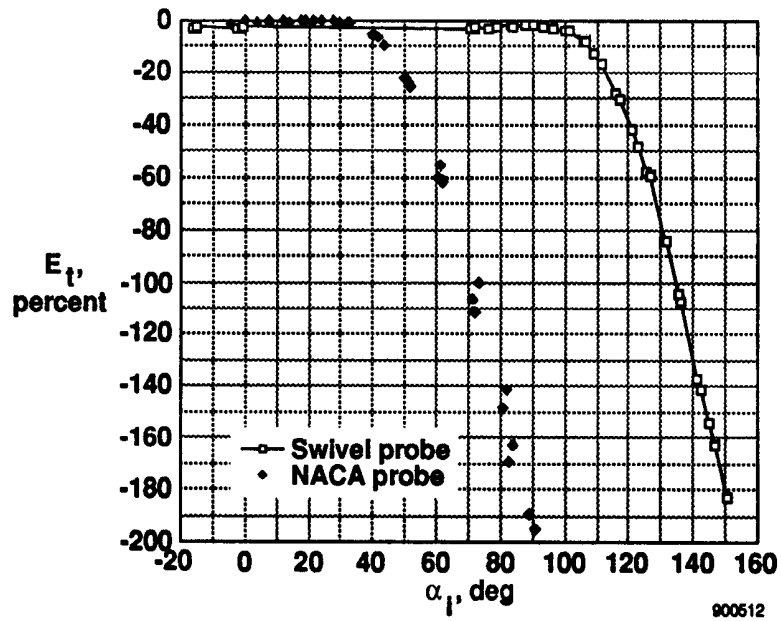


Fig. 19 Swivel-NACA probe total pressure error.

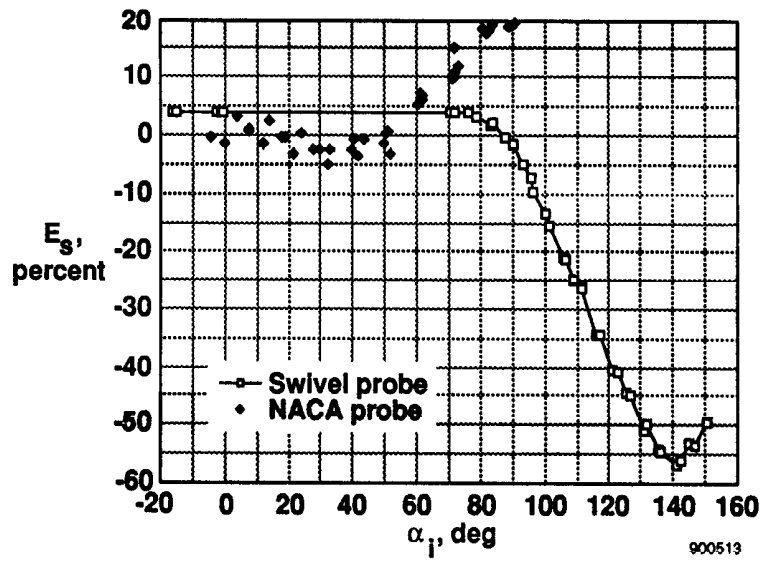


Fig. 20 Swivel-NACA probe static pressure error.